Bbs2-null mice have neurosensory deficits, a defect in social dominance, and retinopathy associated with mislocalization of rhodopsin

Darryl Y. Nishimura*†, Melissa Fath*†, Robert F. Mullins†‡, Charles Searby*§, Michael Andrews*§, Roger Davis*§, Jeaneen L. Andorf‡, Kirk Mykytyn¶, Ruth E. Swiderski*, Baoli Yang‖, Rivka Carmi**, Edwin M. Stone‡§, and Val C. Sheffield*§††

*Department of Pediatrics, Division of Medical Genetics, Departments of ‡Ophthalmology and ‖Obstetrics and Gynecology, and §Howard Hughes Medical Institute, University of Iowa, Iowa City, IA 52242; ¶Department of Pharmacology and Division of Human Genetics, Ohio State University, Columbus, OH 43210; and **Genetic Institute, Soroka Medical Center, Ben Gurion University of the Negev, Beer-Sheva 84101, Israel

Edited by Jeremy Nathans, The Johns Hopkins University School of Medicine, Baltimore, MD, and approved October 7, 2004 (received for review July 28, 2004)

Bardet–Biedl syndrome (BBS) is a heterogeneous, pleiotropic human disorder characterized by obesity, retinopathy, polydactyly, renal and cardiac malformations, learning disabilities, hypogenitalism, and an increased incidence of diabetes and hypertension. No information is available regarding the specific function of BBS2. We show that mice lacking *Bbs2* gene expression have major components of the human phenotype, including obesity and retinopathy. In addition, these mice have phenotypes associated with cilia dysfunction, including retinopathy, renal cysts, male infertility, and a deficit in olfaction. With the exception of male infertility, these phenotypes are not caused by a complete absence of cilia. We demonstrate that BBS2 retinopathy involves normal retina development followed by apoptotic death of photoreceptors, the primary ciliated cells of the retina. Photoreceptor cell death is preceded by mislocalization of rhodopsin, indicating a defect in transport. We also demonstrate that *Bbs2*$^{-/-}$ mice and a second BBS mouse model, *Bbs4*$^{-/-}$, have a defect in social function. The evaluation of *Bbs2*$^{-/-}$ mice indicates additional phenotypes that should be evaluated in human patients, including deficits in social interaction and infertility.

Bardet–Biedl syndrome | mouse model | obesity

Bardet–Biedl syndrome [BBS, Online Mendelian Inheritance in Man (OMIM) 209900] is a genetically heterogeneous disorder characterized by obesity, pigmentary retinopathy, polydactyly, renal malformations, learning disabilities, and hypogenitalism (1–3). Patients also have an increased incidence of diabetes mellitus, hypertension, and congenital heart disease (1, 4, 5). Eight BBS loci have been mapped, and the causative gene at each of these loci has been identified (6–15). Complex inheritance of BBS has been proposed (16). Further study of BBS is likely to provide insight into mechanisms by which Mendelian disorders are modified.

Little is known about the pathophysiology of BBS and the function of BBS proteins. BBS6 is caused by mutations in the *MKKS* gene (8, 9), mutations in which also cause McKusick–Kaufman syndrome (MKKS) (17, 18). MKKS has sequence homology to a prokaryotic chaperonin complex with similarity to a eukaryotic chaperonin, TRiC (17, 19). The other BBS proteins have no significant similarity to chaperonins. BBS4 and BBS8 contain tetratricopeptide repeat domains indicating interaction with other proteins. The recently identified *BBS3* gene codes for an ADP-ribosylation factor-like protein (ARL6) (14, 15).

Several pieces of evidence suggest that BBS genes play a role in cilia function. Except for *BBS6*, BBS genes are expressed in ciliated organisms and not in nonciliated organisms (13, 14, 20). BBS8 localizes to the basal body of ciliated cells (12) and BBS4 localizes to the centriolar satellites of centrosomes and basal bodies of primary cilia (21). We recently demonstrated that spermatozoa of *Bbs4*$^{-/-}$ mice lack flagella, but the absence of Bbs4 does not prevent formation of cilia in general (20). Furthermore, we demonstrated that photoreceptor cells differentiate in the absence of *Bbs4* expression although photoreceptors subsequently underwent apoptosis (20). Collectively, these results support the hypothesis that BBS proteins are involved in ciliary function, but not general cilia assembly.

We now describe a knockout mouse model for BBS2 (*Bbs2*$^{-/-}$). The absence of *Bbs2* gene expression leads to retinal degeneration through apoptosis, failure of flagella formation, obesity associated with increased food intake, and development of renal cysts. In addition, neurological screening reveals deficits including olfactory abnormalities and a defect in social dominance. We show that these phenotypes are likely to be general BBS-associated abnormalities by also demonstrating their presence in *Bbs4*$^{-/-}$ mice.

Materials and Methods

Generation of *Bbs2* Knockout Mice. PCR was used to amplify 5′ and 3′ regions of the *Bbs2* gene from 129/SvJ genomic DNA that were cloned into the targeting vector pOSDUPDEL (provided by O. Smithies, University of North Carolina, Chapel Hill). The linearized vector was electroporated into R1 embryonic stem (ES) cells (129 × 1/SvJ3 129S1/Sv). G418-resistant clones were screened by PCR to identify *Bbs2*-targeted ES cell lines. Two ES cell lines were used to produce chimeras. Mice were genotyped by PCR using primers that both flanked and were internal to the targeted region of the gene (Fig. 1).

Morphological Analysis. For light microscopy, tissues and organs were fixed by immersion in a solution of 4% paraformaldehyde and processed as described (20, 22). *Bbs2*$^{+/+}$ littermates from each time point were used as controls. Testes and trachea were fixed in half-strength Karnovsky's fixative (23) for several hours before osmium postfixation, dehydration, and embedment in Epon 812. Transmission electron micrographs were taken at ×35,000 and ×2,500 through the tracheal cilia and sperm flagella. Retinas (5 months) were processed as described above, and photomicrographs were collected at ×3,000 to ×40,000. Kidneys from *Bbs2*$^{-/-}$ and control mice were fixed as above and processed for scanning electron microscopy.

RNA Isolation and Northern Blot Analysis. Total cellular RNA extraction, poly(A) RNA isolation, electrophoresis, blotting, hybrid-

This paper was submitted directly (Track II) to the PNAS office.

Abbreviations: BBS, Bardet–Biedl syndrome; ES, embryonic stem; ERG, electroretinogram; BMI, body mass index; ONL, outer nuclear layer; TUNEL, terminal deoxynucleotidyltransferase-mediated dUTP nick end labeling; IFT, intraflagellar transport.

†D.Y.N., M.F., and R.F.M. contributed equally to this work.

††To whom correspondence should be addressed. E-mail: val-sheffield@uiowa.edu.

www.pnas.org/cgi/doi/10.1073/pnas.0405496101

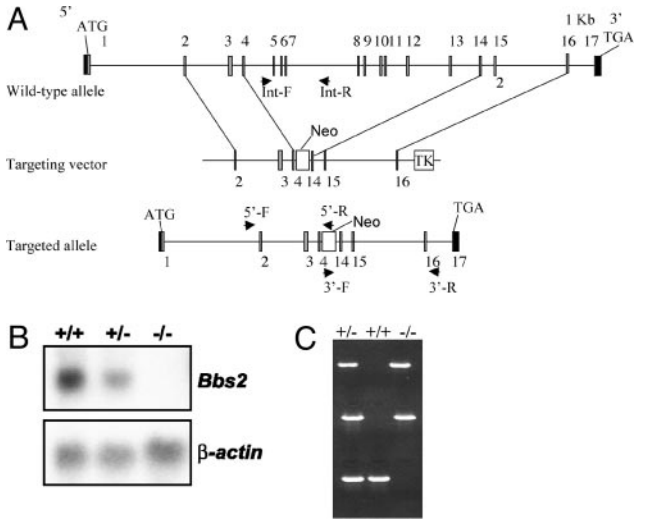

Fig. 1. *Bbs2* gene targeting. (*A*) Strategy for the targeted deletion of *Bbs2*. Upon homologous recombination, exons 5–14 are replaced with a neomycin cassette. (*B*) (*Upper*) Northern blot analysis of *Bbs2* expression in kidney total cellular RNA from WT (+/+), heterozygous (+/−), and homozygous (−/−) animals. The probe is a *Bbs2* partial 3′ cDNA. (*Lower*) The same blot probed with β-actin as a loading control. (*C*) PCR genotyping of heterozygous (+/−), WT (+/+), and homozygous (−/−) mice. The top and middle amplimers correspond to 5′ and 3′ regions of the neomycin resistance gene, respectively. The bottom band is derived from amplification with *Bbs2* internal primers.

ization, and autoradiography were carried out as described (24). Total RNA (10 μg) from BALB/c whole brain and discrete regions were purchased from BD Biosciences/Clontech. A mouse (ICR) embryo full-stage blot was purchased from Seegene (Seoul, Korea), and an adult multiple tissue Northern blot was purchased from Clontech. Probes were labeled with [^{32}P]-dCTP.

Electroretinography. Electroretinography was performed on *Bbs2*$^{-/-}$ and control mice at 10 weeks and 5 months of age. Electroretinograms (ERGs) were collected by using a Ganzfeld bowl equipped with a PS33 Plus photic stimulator from dark-adapted mice after anesthesia. Electrophysiologic data after flash stimulation were collected by using ERG tool software (courtesy of Richard Weleber, Oregon Health & Science University, Portland).

Weight Studies. Animals were weighed at 3 and 4 weeks of age and monthly thereafter. For feeding studies, a fixed weight of food was added to each cage containing a single animal, and the remaining food was weighed daily.

Primary Behavioral Observation Screen. The primary observation screen is a modification of the SHIRPA protocol (see www.mgc.har.mrc.ac.uk/mutabase and ref. 25). Data from 38 separate observations were quantified and recorded for each animal. Assessment of each animal began with observation of motor behavior, followed by assessment of vision, grip strength, righting reflex, negative geotaxis, body tone, reflexes, limb tone, provoked biting, and salivation. Incidences of abnormal behavior, fear, irritability, aggression, or vocalization were recorded. Five male and 10 female *Bbs2*$^{-/-}$ mice and their age-matched heterozygote and WT controls were evaluated. Similar numbers of *Bbs4*$^{-/-}$, heterozygote, and WT mice were evaluated. Observers were masked to the genotyping data.

Social Dominance Tube Test. Thirty-three *Bbs2* WT, heterozygote, and knockout mice (four males and seven females each) were tested as described (26) in a 30 cm long × 3.0 cm diameter tube. Two age- and gender-matched mice of different genotypes were released toward each other from opposite ends of the tube. A subject was declared a "winner" when its opponent backed out of the tube. Each pairing was performed twice for a total of 66 trials. Thirty *Bbs*4 mice were tested in a similar manner.

Olfactory Test. Thirteen WT, heterozygote, and *Bbs2*$^{-/-}$ mice (six males and seven females each) were tested as described (27). Briefly, the time required (up to a maximum of 20 min) for fasted mice to locate a hidden piece of Doritos (Frito-Lay, Dallas) nacho corn chip was determined. Similarly, 16 *Bbs4*-null mice (10 females and 6 males) were tested along with heterozygote and WT controls.

Data Analysis. Significance was determined by using χ^2 analysis. Where appropriate (i.e., scaled data from the primary behavioral observations), nonparametric analyses were conducted by using Fisher's exact test. Tobit's analysis was used for right censored olfactory data.

Results

Generation of Bbs2-Deficient Mice. We generated a gene-targeting construct designed to remove exons 5–14 (Fig. 1), transfected the construct into ES cells, and identified five homologous recombinants by genotyping 1,056 ES cell lines (0.5%). Two targeted clones were used to produce chimeras. Chimeric mice were used to generate *Bbs2* heterozygous (*Bbs2*$^{+/-}$) mice on mixed and inbred genetic backgrounds by mating with C57BL/6J and 129/SvEv mice, respectively. *Bbs2*$^{+/-}$ mice were mated, and genotyping of litters from *Bbs2*$^{+/-}$ intercrosses indicated that *Bbs2*$^{-/-}$ offspring were fewer than the predicted Mendelian ratios ($P < 0.001$). *Bbs2* targeting resulted in a null allele as demonstrated by the complete absence of *Bbs2* mRNA by Northern analysis (Fig. 1).

***Bbs2* Expression.** A Northern blot of total cellular RNA isolated from mouse embryos was hybridized with a ^{32}P-labeled *Bbs2* probe. Embryo samples from 4.5–6.5 embryonic days postconception include extraembryonic tissues and maternal uterus. As seen in Fig. 2*A*, *Bbs2* gene expression was detectable very early during mouse embryogenesis, although possible maternal contribution to *Bbs2* gene expression cannot be excluded during the earliest time points. *Bbs2* expression continued throughout embryogenesis.

Ubiquitous *Bbs2* RNA expression in variable abundance was observed in adult mouse tissues (Fig. 2*B*). *Bbs2* is abundantly expressed in heart, brain, kidney, testis, and eye. Moderate expression was noted in adult lung, liver, and adipose tissue. Low levels of expression were seen in spleen and skeletal muscle and in the pancreas (7). In addition to the 3-kb *Bbs2* mRNA, at least two larger transcripts (5 and 4 kb) were observed in some tissues, suggesting incompletely processed *Bbs2* nuclear RNAs. *Bbs2* gene expression was seen in variable abundance throughout discrete regions of the mouse and human brain (Fig. 2*C*). Widespread *BBS2* gene expression was also seen in the human brain by Northern blotting (R.E.S. and V.C.S., unpublished data).

***Bbs2*$^{-/-}$ Mice Become Obese.** *Bbs2*$^{-/-}$ mice were grossly normal with respect to morphology. *Bbs2*$^{-/-}$ mice are smaller at birth and at weaning than their littermates. By 12 weeks, *Bbs2*$^{-/-}$ mice weigh the same as *Bbs2*$^{+/+}$ and *Bbs2*$^{+/-}$ animals (Fig. 3). By 4 months, both weight and body mass index (BMI; kg/M^2) are significantly greater in *Bbs2*$^{-/-}$ female mice compared with *Bbs2*$^{+/+}$ female mice ($P < 0.01$). By 5 months, *Bbs2*$^{-/-}$ male animals show a modest but significant weight gain compared with WT animals. The increase in weight is associated with an increase in abdominal fat. Longitudinal feeding studies indicate that *Bbs2*$^{-/-}$ mice eat more than their littermates. The increase in food intake begins in young animals and continues in older mice (Fig. 3).

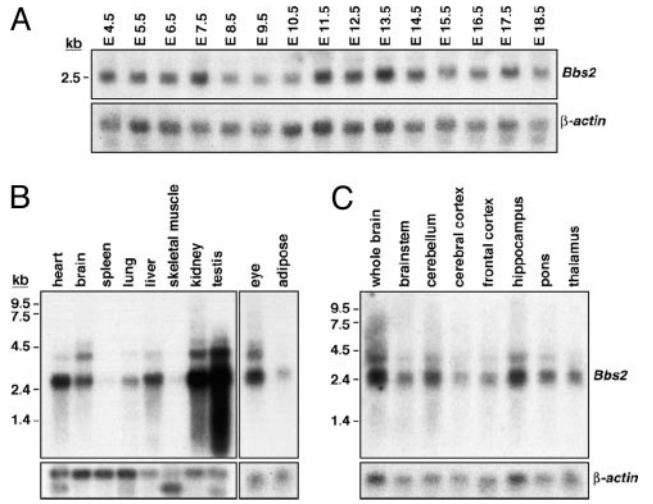

Fig. 2. *Bbs2* gene expression. (*A*) Northern blot analysis of mouse *Bbs2* RNA (20 μg) isolated from embryos 4.5 embryonic days postconception (E4.5) through E18.5 demonstrates early and widespread *Bbs2* expression. The blot was sequentially hybridized with ^{32}P-labeled *Bbs2* and β-actin probes. (*B*) Northern blot analysis of *Bbs2* gene expression in adult mouse tissues. Poly(A) mRNA (2 μg) was sequentially hybridized with ^{32}P-labeled *Bbs2* and β-actin probes. (*C*) Northern blot analysis of *Bbs2* gene expression in discrete regions of the adult mouse brain. Total RNA (10 μg) was sequentially hybridized with ^{32}P-labeled *Bbs2* and β-actin probes.

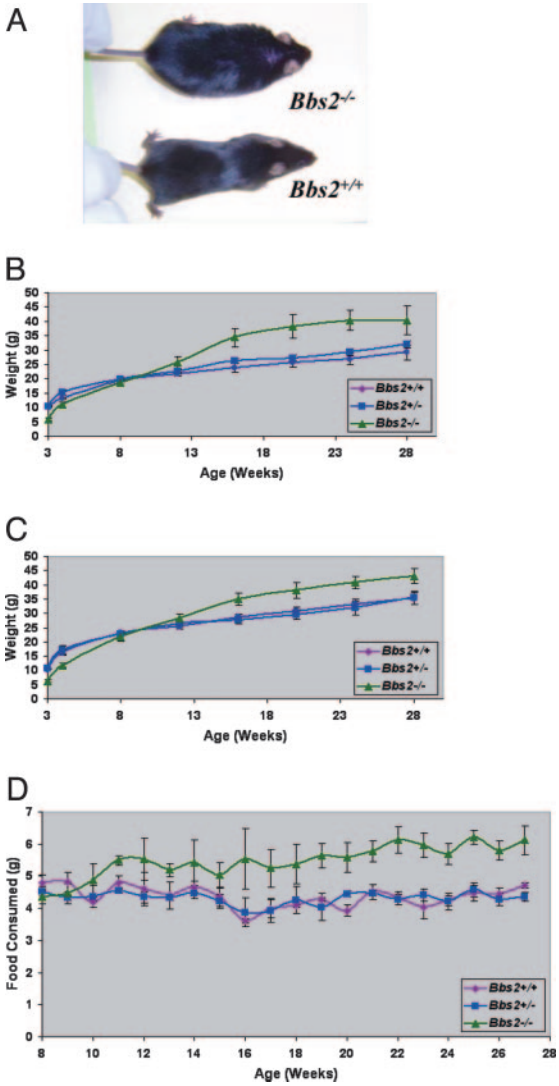

Fig. 3. Weight gain and food consumption of $Bbs2^{+/+}$, $Bbs2^{+/-}$, and $Bbs2^{-/-}$ mice. (*A*) Photograph depicting typical obesity phenotype of $Bbs2^{-/-}$ mice. (*B*) *Bbs2* female weight versus age comparison (minimum of five animals per group). (*C*) Weight versus age for all animals (males and females combined with a minimum of 10 mice per group). $Bbs2^{-/-}$ mice are statistically different from $Bbs2^{+/+}$ and $Bbs2^{+/-}$ mice. (*D*) *Bbs2* average food consumed (males and females combined with a minimum of six animals per group). Food consumption was averaged every 7 days.

***Bbs2*$^{-/-}$ Mice Mislocalize Rhodopsin and Display Photoreceptor Apoptotic Cell Loss.** $Bbs2^{-/-}$ mice appear to have normal retinas early in life, but subsequently undergo retinal degeneration. At 6–8 weeks, $Bbs2^{-/-}$ mice have a significant degree of retinal degeneration at the level of the outer nuclear layer (ONL) (Fig. 4). At 5 months, the $Bbs2^{-/-}$ animals retained some ONL photoreceptor nuclei and some remnants of inner and outer segments. In some areas, the retinal pigment epithelium overlying the degenerating photoreceptors appeared detached and discontinuous with pigment migration into the outer retina. The inner nuclear layer, outer plexiform layer, and ganglion cell layer appeared normal at all ages examined. By 10 months, the ONL was completely absent with an intact inner retina.

Antirhodopsin staining of the retinas of $Bbs2^{-/-}$ animals before loss of photoreceptors revealed opsin immunoreactivity between the retinal pigment epithelium and ONL (Fig. 5). Notably, rhodopsin was localized to some cell bodies in the ONL (Fig. 5*B*, arrows).

$Bbs2^{-/-}$ mice had multiple-labeled terminal deoxynucleotidyltransferase-mediated dUTP nick end labeling (TUNEL)-positive nuclei in the ONL per high-power field, whereas TUNEL-positive nuclei were rarely seen in littermates. These results demonstrate that photoreceptor cells of $Bbs2^{-/-}$ mice undergo retinal degeneration through apoptosis (Fig. 5*D*).

To determine whether mislocalization of rhodopsin preceded or was concurrent with photoreceptor cell death, we compared the results of the TUNEL assay with the pattern of rhodopsin labeling. In general, cell bodies that were labeled with antirhodopsin antibody were not TUNEL-positive, and the number of apoptotic cells was much smaller than the number of rhodopsin-labeled cells. Immunohistochemical labeling of rds and Rom1 was also performed in 5-month $Bbs2^{-/-}$ retinas. Immunolabeling was restricted to the inner/outer segments, which are poorly differentiated in these animals. Labeling of photoreceptor cell bodies was not obvious with these antibodies by epifluorescence microscopy (data not shown).

Ultrastructural analyses of the eyes from a 5-month-old $Bbs2^{-/-}$ mouse revealed highly disorganized photoreceptor outer segments, as compared with the neatly organized stacks of membranous disks in WT animals. Whorls of membranes were present in the subretinal space, without any evidence of parallel membrane stacks. Connecting cilia were rarely observed in the 5-month-old $Bbs2^{-/-}$ mice (Fig. 5 *E* and *F*).

To determine whether histological abnormalities correlated with electrophysiological function in the *Bbs2*-deficient mice, electroretinography was performed. A severe attenuation of rod and cone responses was noted on electrophysiological recordings of light- and dark-adapted mice, as compared with controls (Table 2, which is published as supporting information on the PNAS web site). In contrast to the histological findings, in which the ONL is reduced but still patent at 10 weeks of age, the ERG waveforms reveal a major decline in photoreceptor function at 10 weeks (Fig. 7, which is published as supporting information on the PNAS web site). By 5 months of age, no detectable signal was obtained from $Bbs2^{-/-}$ mice.

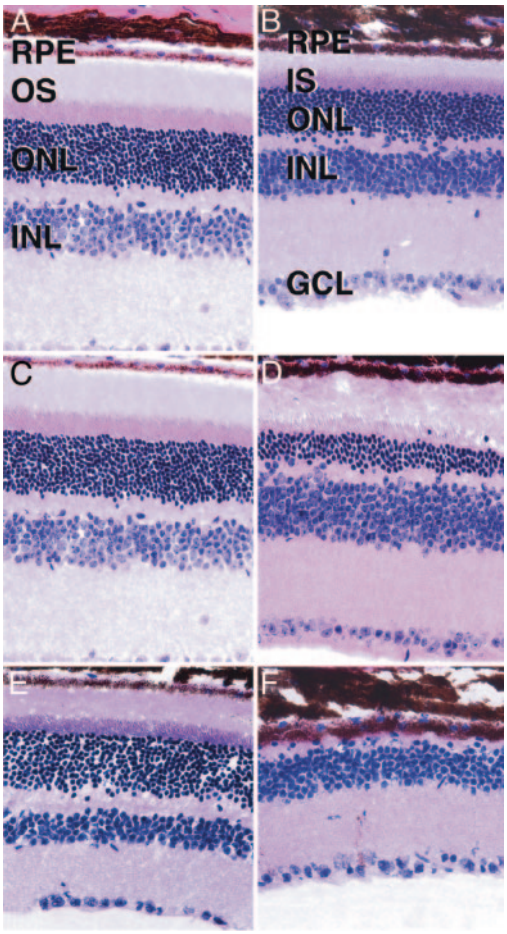

Fig. 4. Hematoxylin/eosin staining of age-matched *Bbs2*$^{+/+}$ (*A*, *C*, and *E*) and *Bbs2*$^{-/-}$ (*B*, *D*, and *F*) mouse retinas. Mice were examined at 7 weeks (*A* and *B*), 5 months (*C* and *D*), and 10 months (*E* and *F*). Some degenerative changes in the ONL are apparent in 7-week-old mice, although inner and outer segments are clearly distinguishable. By 5 months of age (*C* and *D*), the distinction between inner and outer segments is less apparent and the ONL is significantly thinner than in *Bbs2*$^{+/+}$ eyes. At 10 months of age (*E* and *F*), the ONL is largely degenerated and no inner or outer segments are present. RPE, retinal pigment epithelium; IS, inner segments; OS, outer segments; INL, inner nuclear layer; GCL, ganglion cell layer. (Magnification: ×160.)

***Bbs2*$^{-/-}$ Mice Fail to Form Flagella, and Human Patients Have Abnormal Spermatozoa.** Male *Bbs2*$^{-/-}$ animals appear to be infertile. To investigate the reason for the male infertility, we performed histological analysis on testes from *Bbs2*$^{-/-}$ male animals. Although nuclei with highly condensed chromatin resembling spermatozoa heads were present, flagella were completely absent (Fig. 6).

Semen samples from two adult male BBS2 patients were examined. Both patients were homozygous for the same missense mutation (V75G) and were from the extended pedigree used to initially identify the *BBS2* gene (7). Quantitative semen analysis of both patients, using scanning and transmission electron microscopy, revealed severe oligoteratoastenozoospermia with severe necrozoospermia and severe abnormalities of the sperm acrosome, nucleus, and axonemal structures (data not shown).

***Bbs2*$^{-/-}$ Mice Have Tracheal Cilia.** Ultrastructural analysis of tracheal cilia revealed a grossly normal 9-plus-2 pattern of microtubules in *Bbs2*$^{+/+}$ and *Bbs2*$^{-/-}$ mice (Fig. 6*C*). Of note, a fraction of *Bbs2*$^{-/-}$ cilia appeared to possess abnormalities resembling vesicles associated with the central pair of microtubules in one *Bbs2*$^{-/-}$ mouse (Fig. 6*D*). The majority of the cilia appeared normal by transmission electron microscopy (data not shown).

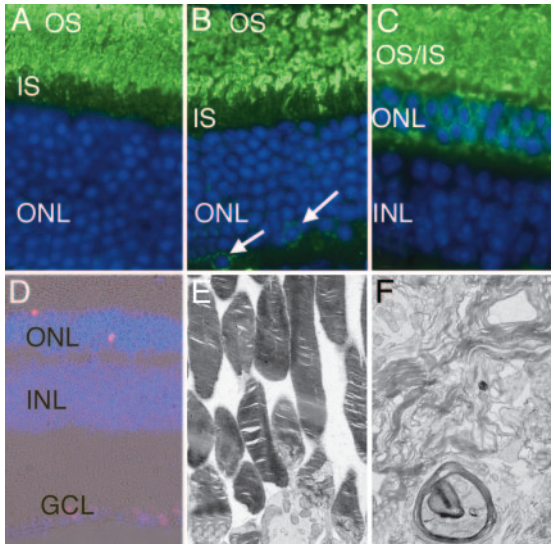

Fig. 5. Localization of rhodopsin in 7-week *Bbs2*$^{+/+}$ (*A*), 7-week *Bbs2*$^{-/-}$ (*B*), and 5-month *Bbs2*$^{-/-}$ (*C*) mice. (*A*) In *Bbs2*$^{+/+}$ retinas, rhodopsin (green) is largely confined to the outer segments (OS), with little labeling of inner segments (IS). (*B*) *Bbs2*$^{-/-}$ mice at 7 weeks of age also predominantly localize rhodopsin to the OS, although some cell bodies in the ONL also appear to be labeled (arrows). (*C*) At 5 months of age *Bbs2*$^{-/-}$ mice do not exhibit partitioning of rhodopsin between the IS and OS. Labeling of ONL cell bodies is readily apparent. Photoreceptor degeneration in the *Bbs2*$^{-/-}$ mouse is caused by apoptosis as revealed by TUNEL labeling of the ONL (*D*, red). Ultrastructural analysis of *Bbs2*$^{-/-}$ mouse retina at 5 months of age reveals membranous whorls in the subretinal space (*F*) as compared with the orderly arrangement of membranous disks in *Bbs2*$^{+/-}$ (*E*) and WT mice. (Magnification: ×380, *A–C*; ×110, *D*; and ×3,000, *E* and *F*.)

***Bbs2*$^{-/-}$ Mice Develop Renal Cysts.** Three 5-month-old animals were killed and examined for renal abnormalities. Two of the three animals had bilateral multicystic kidneys (Fig. 6*F*). Several cysts were found in the urinary space surrounding glomeruli. Primary cilia were present on renal tubular cells in *Bbs2*$^{-/-}$ mice, although some cilia do not appear to be normal in shape compared with cilia of WT animals (Fig. 6 *G* and *H*).

Histology of the livers of 5-month-old *Bbs2*$^{-/-}$ knockout mice revealed lipid accumulation, but there was no evidence of hepatic cysts.

Although polydactyly is a common feature of BBS in humans, no *Bbs2*$^{-/-}$ mice had polydactyly or other notable limb abnormalities.

Neurosensory and Behavioral Phenotypes. Data from 38 separate observational measurements were compared among *Bbs2*$^{+/+}$, *Bbs2*$^{+/-}$, and *Bbs2*$^{-/-}$ mice and those with significant differences are summarized in Table 1. There were no significant differences when comparing the data from *Bbs2*$^{+/-}$ with *Bbs2*$^{+/+}$ mice of either sex. There were no significant differences in the observations that assess muscle and lower motor neuron functions and in some of the observations to assess sensory functions such as toe pinch and reflexes. There was a significant difference in touch escape, with *Bbs2*$^{-/-}$ mice being less sensitive to touch ($P < 0.0001$). *Bbs2*$^{-/-}$ mice also showed a decreased response to acoustic startle ($P < 0.05$). There was a significant effect of genotype on visual placing with *Bbs2*$^{-/-}$ female mice showing less forelimb grasping ($P < 0.05$). *Bbs2*$^{-/-}$ mice were less vocal during handling ($P < 0.0001$) and showed diminished olfaction as measured by the ability to find hidden food ($P < 0.001$).

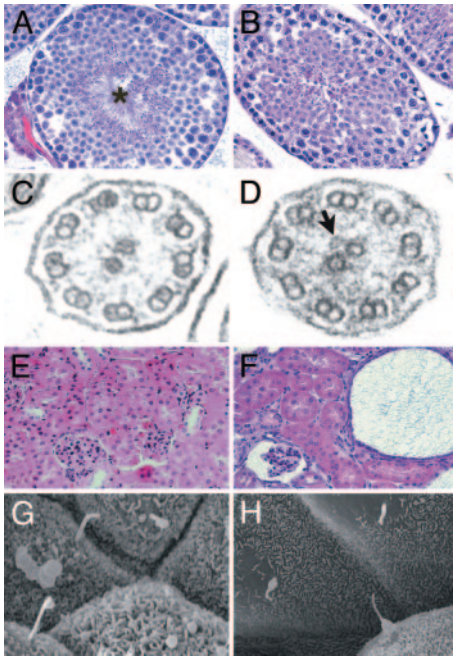

Fig. 6. Hematoxylin/eosin-stained sections of the testes of *Bbs2*$^{+/+}$ (*A*) and *Bbs2*$^{-/-}$ (*B*) mice show that, whereas WT mice possess numerous flagella in the seminiferous tubules (*), the *Bbs2*$^{-/-}$ mice have no flagella. Some condensed chromatin, indicating spermatogenesis, is detectable. Transmission electron micrographs through the tracheal cilia of *Bbs2*$^{+/+}$ (*C*) and *Bbs2*$^{-/-}$ (*D*) mice reveal a normal 9- plus -2 pattern of microtubules. In some cases, vesicles were observed in association with these microtubules in *Bbs2*$^{-/-}$ mice (*C*, arrow). Kidneys from *Bbs2*$^{+/+}$ (*E*) and *Bbs2*$^{-/-}$ (*F*) mice are shown. *Bbs2*$^{-/-}$ mice have numerous cysts, some of which involve the glomerulus. Scanning electron microscopic views of renal tubules from *Bbs2*$^{+/+}$ (*G*) and *Bbs2*$^{-/-}$ (*H*) mice showing primary cilia. Some cells from *Bbs2*$^{-/-}$ mice show abnormally tapered cilia. (Magnification: ×100, *A* and *B*; ×90,000, *C* and *D*; ×90, *E* and *F*; and ×2,500 *G* and *H*.)

Because *Bbs2*$^{-/-}$mice were more docile to handling, a social dominance tube test was performed by pairing same-gender mice (26). In 19 of 22 trials (86%), *Bbs2*$^{+/+}$ mice won when tested against *Bbs2*$^{-/-}$ mice ($P < 0.01$). When *Bbs2*$^{+/-}$ mice were tested against *Bbs2*$^{-/-}$ mice, the *Bbs2*$^{+/-}$ mice won 19 of 22 trials (86%) ($P < 0.01$). Both male and female *Bbs2*$^{-/-}$ mice lost more bouts than expected by chance, demonstrating that *Bbs2*$^{-/-}$ mice are more submissive than controls. There was no difference in social dominance between *Bbs2*$^{+/+}$ and *Bbs2*$^{+/-}$ animals.

Table 1. Summary of phenotype differences between *Bbs2*$^{-/-}$ and *Bbs4*$^{-/-}$ mice compared with WT littermates in SHIRPA primary screen of behavioral observations

	Phenotype		
Behavior	*Bbs2*$^{-/-}$	*Bbs4*$^{-/-}$	WT
Touch escape	0 ($P < 0.0001$)	0 ($P < 000005$)	1
Startle response	1 ($P < 0.05$)	2 ($P > 0.05$)	2
Wire maneuver	0 ($P > 0.05$)	2 ($P < 0.005$)	0
Salivation	1 ($P < 0.05$)*	0 ($P < 0.005$)	2
Vocalization	0 ($P < 0.0001$)	0 ($P < 0.01$)	1
Olfaction	11.8 min ($P < 0.005$)	11.4 min ($P < 0.0001$)	2.6 min

Data are presented as mode with *P* value determined by Fisher's exact test in parentheses. Only phenotypes displaying a significant difference ($P < 0.05$) in at least one knockout mouse line (either *Bbs2*$^{-/-}$ or *Bbs4*$^{-/-}$) are presented.
*Significant in females only.

Evaluation of *Bbs4*$^{-/-}$ Mice Confirm BBS-Associated Neurosensory Phenotypes. To determine whether the neurosensory and social dominance phenotypes were specific to *Bbs2* deficiency or, alternatively, were general BBS phenotypes, *Bbs4*$^{-/-}$ mice were also screened for 38 observational measurements. *Bbs4*$^{-/-}$ mice showed deficits in visual placement, olfaction, vocalization, and touch escape (Table 1), the same phenotypes for which *Bbs2*$^{-/-}$ animals showed deficits. Social dominance testing revealed that *Bbs4*$^{-/-}$ mice were less dominant than either WT or heterozygous mice, losing 95% of trials ($P < 0.001$).

Evaluation of Complex Inheritance in BBS Mice. It has been postulated that in some cases a third mutation (at a second locus) is required for penetrance of BBS in humans (16). In this study, all *Bbs2*$^{-/-}$ mice developed retinal degeneration as determined by fundus photography and ERG or histological examination. There was no evidence of incomplete penetrance of the retinal phenotype in *Bbs2*$^{-/-}$ animals, a finding consistent with recessive inheritance. *Bbs2*$^{-/-}$ mice weigh significantly more and have a significantly higher BMI than control animals, although there is variability between the weights and BMI of same-gender animals. The polycystic kidney component of the phenotype does not appear to be fully penetrant. Double heterozygous animals (*Bbs2*$^{+/-}$*Bbs4*$^{+/-}$) have been generated at the predicted Mendelian ratios from *Bbs2*$^{+/-}$ × *Bbs4*$^{+/-}$ matings. These mice are normal with respect to weight, BMI, ERG, fundus photography, retinal histology, limb development, and fertility.

Discussion

The findings described here contribute to the understanding of the pathogenesis and genetics of BBS and suggest unique BBS-associated phenotypes that should be evaluated in humans. We show that *Bbs2*$^{-/-}$ mice develop obesity and retinal degeneration, and in males, fail to synthesize flagella. In addition, these animals have polycystic kidney disease, olfactory dysfunction, and a behavioral phenotype suggesting abnormal social interaction.

Based on localization of some BBS proteins to the basal body of ciliated cells (12, 21), BBS proteins could be involved in ciliogenesis, cilia maintenance, intraciliary transport [often referred to as intraflagellar transport (IFT)], and/or intracellular transport. The results reported here for *Bbs2*$^{-/-}$ animals and previously for *Bbs4*$^{-/-}$ animals (20) indicate that neither the Bbs2 nor Bbs4 proteins are absolutely required for initial cilia assembly. This finding is demonstrated by the fact that functioning and morphologically normal photoreceptors with connecting cilia are present in young *Bbs2*$^{-/-}$ and *Bbs4*$^{-/-}$ mice and the finding of morphologically normal-appearing cilia in the trachea of knockout mice. Although the outer segments of the photoreceptors appear to develop normally, they become disorganized and eventually undergo apoptosis.

We hypothesize that the absence of Bbs2 injures the photoreceptor cell by compromising the intracellular transport and IFT requirements for maintenance of the rapidly regenerating outer segments. To investigate this hypothesis, we labeled retinas from control and *Bbs2*$^{-/-}$ mice with antirhodopsin antibody. Of note, rhodopsin was found to accumulate in the photoreceptor cell bodies in *Bbs2*$^{-/-}$ retinas, demonstrating mislocalization of rhodopsin. The mislocalization of rhodopsin precedes apoptosis, as cells displaying mislocalization were far more abundant than cells that were TUNEL-positive and were distributed differently than the TUNEL-positive cells. These data support a role for BBS2 in intracellular transport and IFT.

Opsins appear to be found in the outer segments, indicating that a complete defect in antegrade IFT does not occur. The mislocalization of rhodopsin to cell bodies of the ONL has been described in other forms of murine retinal degeneration (28). The lack of detectable Rom1 and rds/peripherin in the cell bodies may indicate that either Bbs2 must be functional for the trafficking of some, but

not other, outer segment proteins, or that the level of detection of these less abundant proteins was less robust than for the highly abundant rhodopsin protein. The finding of accumulation of vesicles in cilia in this study further indicates that IFT is compromised.

A striking exception to the apparent need for BBS proteins for cilia assembly is the assembly of flagella. The failure of flagella formation during spermatogenesis indicates that there are differences between the processes or demands of flagella compared to cilia assembly. We also demonstrated that human BBS2 patients had impaired spermatogenesis, although some flagella were present. This finding indicates that in some circumstances flagella formation can occur in the absence of a functioning BBS2 protein or that the missense mutation does not result in a completely nonfunctional BBS2 protein.

Of note, *Bbs2*$^{-/-}$ animals can assemble primary cilia of renal tubule cells, although these cilia appear to be tapered. Further study of renal tubule cells is required to determine the exact nature of the cilia abnormality. The development of renal cysts in *Bbs2*$^{-/-}$ animals suggests a defect in mechanosensation by primary cilia of renal tubular cells, because such a mechanism is known to cause polycystic kidney disease (29). These cumulative data indicate involvement of motor, sensory, and mechanosensory cilia in BBS.

Differences between the BBS phenotype and the phenotype that is commonly attributed to defects in motile cilia indicate that the BBS phenotype cannot be explained solely by disruption of cilia motility. Patients with primary ciliary dysfunction, such as Kartagener syndrome, commonly have bronchiectasis and sinusitis, whereas these symptoms are not recognized as common features of BBS, although an increased incidence of asthma has been suggested in patients with BBS. There was no direct evidence of lung disease or situs abnormalities in the *Bbs2*$^{-/-}$ mice examined in this study.

Our data indicate that *Bbs2*$^{-/-}$ mice develop obesity associated with increased food consumption that begins before the onset of obesity. Based on these data, it would appear that *Bbs2*$^{-/-}$ mice have a defect in regulation of satiety. The presence of obesity may indicate a previously unknown connection between ciliary function, IFT and/or intracellular transport, and the maintenance of appropriate body weight. Alternatively, obesity in these animals may result from defects in neuronal development or neuron-specific degeneration.

The finding of neurological deficits in the *Bbs2*$^{-/-}$ mice indicates that neurodevelopment or neurodegenerative abnormalities resulting from *Bbs2* deficiency are not limited to satiety regulation. The results of the social dominance tube test indicate that the knockout mice are less dominant than their littermate controls. This phenotype appears to be a general BBS phenotype, as *Bbs4*$^{-/-}$ animals also have a deficit in social dominance. This phenotype cannot be attributed solely to vision defects because it occurs in young animals (before onset of blindness) and can be replicated in a totally dark environment. Further study of these animals has the potential for determining neuronal pathways involved in social interaction.

We also demonstrated that both *Bbs2*$^{-/-}$ and *Bbs4*$^{-/-}$ mice have deficits in smell. This finding is consistent with the recent report of anosmia in humans and mice (30).

Complex inheritance of BBS has been suggested in humans. The possibility of complex inheritance of BBS has implications for assigning recurrence risks for BBS families and understanding the biochemistry underlying the BBS phenotypes. In mice, some of the observed phenotypes (retinal degeneration) appear to be fully penetrant. These data support the conclusion that BBS is a highly penetrant autosomal recessive disorder with variable expressivity.

The development of Bbs2 and Bbs4 mouse models will allow evaluation of genetic interaction between *Bbs2* and *Bbs4* to determine whether these genes modify each other, particularly with respect to some less penetrant components of the phenotype, such as renal cysts.

It is of interest that *Bbs2*$^{-/-}$ animals do not have all of the components of the human phenotype, most notably polydactyly. The lack of polydactyly is not specific for *Bbs2*-deficient animals, as *Bbs4* knockout animals also do not have polydactyly (20). These data indicate that a fundamental difference exists between the role of BBS proteins in limb development in humans and mice.

We thank K. Bugge, M. Olvera, C. Eastman, G. Beck, R. Burry, A. Fischer, and K. Wolken for technical assistance; D. Aguiar Crouch for administrative assistance; Drs. Robert Molday (University of British Columbia, Vancouver) and Joe Besharse (Medical College of Wisconsin, Milwaukee) for their generous donations of antibodies; Dr. Kai Wang for assistance with the statistical analyses; and the University of Iowa Department of Pathology and Central Electron Microscopy Research Facility for assistance. This work was supported by National Institutes of Health Grants P50-HL-55006 (to V.C.S.) and R01-EY-11298 (to V.C.S. and E.M.S.), Carver Endowment for Molecular Ophthalmology (E.M.S. and V.C.S.), and Research to Prevent Blindness, New York (Department of Ophthalmology, University of Iowa). V.C.S. and E.M.S. are Investigators of the Howard Hughes Medical Institute.

1. Green, J. S., Parfrey, P. S., Harnett, J. D., Farid, N. R., Cramer, B. C., Johnson, G., Heath, O., McManamon, P. J., O'Leary, E. & Pryse-Phillips, W. (1989) *N. Engl. J. Med.* **321,** 1002–1009.
2. Biedl, A. (1922) *Dtsch. Med. Wochenschr.* **48,** 1630.
3. Bardet, G. (1920) Ph.D thesis (University of Paris, Paris).
4. Elbedour, K., Zucker, N., Zalzstein, E., Barki, Y. & Carmi, R. (1994) *Am. J. Med. Genet.* **52,** 164–169.
5. Harnett, J. D., Green, J. S., Cramer, B. C., Johnson, G., Chafe, L., McManamon, P., Farid, N. R., Pryse-Phillips, W. & Parfrey, P. S. (1988) *N. Engl. J. Med.* **319,** 615–618.
6. Mykytyn, K., Braun, T., Carmi, R., Haider, N. B., Searby, C. C., Shastri, M., Beck, G., Wright, A. F., Iannaccone, A., Elbedour, K., *et al.* (2001) *Nat. Genet.* **28,** 188–191.
7. Nishimura, D. Y., Searby, C. C., Carmi, R., Elbedour, K., Van Maldergem, L., Fulton, A. B., Lam, B. L., Powell, B. R., Swiderski, R. E., Bugge, K. E., *et al.* (2001) *Hum. Mol. Genet.* **10,** 865–874.
8. Katsanis, N., Beales, P. L., Woods, M. O., Lewis, R. A., Green, J. S., Parfrey, P. S., Ansley, S. J., Davidson, W. S. & Lupski, J. R. (2000) *Nat. Genet.* **26,** 67–70.
9. Slavotinek, A. M., Stone, E. M., Mykytyn, K., Heckenlively, J. R., Green, J. S., Heon, E., Musarella, M. A., Parfrey, P. S., Sheffield, V. C. & Biesecker, L. G. (2000) *Nat. Genet.* **26,** 15–16.
10. Mykytyn, K., Nishimura, D. Y., Searby, C. C., Shastri, M., Yen, H. J., Beck, J. S., Braun, T., Streb, L. M., Cornier, A. S., Cox, G. F., *et al.* (2002) *Nat. Genet.* **31,** 435–438.
11. Badano, J. L., Ansley, S. J., Leitch, C. C., Lewis, R. A., Lupski, J. R. & Katsanis, N. (2003) *Am. J. Hum. Genet.* **72,** 650–658.
12. Ansley, S. J., Badano, J. L., Blacque, O. E., Hill, J., Hoskins, B. E., Leitch, C. C., Kim, J. C., Ross, A. J., Eichers, E. R., Teslovich, T. M., *et al.* (2003) *Nature* **425,** 628–633.
13. Li, J. B., Gerdes, J. M., Haycraft, C. J., Fan, Y., Teslovich, T. M., May-Simera, H., Li, H., Blacque, O. E., Li, L., Leitch, C. C., *et al.* (2004) *Cell* **117,** 541–552.
14. Chiang, A. P., Nishimura, D., Searby, C., Elbedour, K., Carmi, R., Ferguson, A. L., Secrist, J., Braun, T., Casavant, T., Stone, E. M., *et al.* (2004) *Am. J. Hum. Genet.* **75,** 475–484.
15. Fan, Y., Esmail, M. A., Ansley, S. J., Blacque, O. E., Boroevich, K., Ross, A. J., Moore, S. J., Badano, J. L., May-Simera, H., Compton, D. S., *et al.* (2004) *Nat. Genet.* **36,** 989–993.
16. Katsanis, N., Ansley, S. J., Badano, J. L., Eichers, E. R., Lewis, R. A., Hoskins, B. E., Scambler, P. J., Davidson, W. S., Beales, P. L. & Lupski, J. R. (2001) *Science* **293,** 2256–2259.
17. Stone, D. L., Slavotinek, A., Bouffard, G. G., Banerjee-Basu, S., Baxevanis, A. D., Barr, M. & Biesecker, L. G. (2000) *Nat. Genet.* **25,** 79–82.
18. Robinow, M. & Shaw, A. (1979) *J. Pediatr.* **94,** 776–778.
19. Frydman, J., Nimmesgern, E., Erdjument-Bromage, H., Wall, J. S., Tempst, P. & Hartl, F. U. (1992) *EMBO J.* **11,** 4767–4778.
20. Mykytyn, K., Mullin, R. F., Andrews, M., Chiang, A. P., Swiderski, R. E., Yang, B., Braun, T., Casavant, T., Stone, E. M. & Sheffield, V. C. (2004) *Proc. Natl. Acad. Sci. USA* **101,** 8664–8669.
21. Kim, J. C., Badano, J. L., Sibold, S., Esmail, M. A., Hill, J., Hoskins, B. E., Leitch, C. C., Venner, K., Ansley, S. J., Ross, A. J., *et al.* (2004) *Nat. Genet.* **36,** 462–470.
22. Johnson, L. V. & Blanks, J. C. (1984) *Curr. Eye Res.* **3,** 969–974.
23. Russell, S. R., Mullins, R. F., Schneider, B. L. & Hageman, G. S. (2000) *Am. J. Ophthalmol.* **129,** 205–214.
24. Swiderski, R. E., Ying, L., Cassell, M. D., Alward, W. L., Stone, E. M. & Sheffield, V. C. (1999) *Mol. Brain Res.* **68,** 64–72.
25. Rogers, D., Fisher, E., Brown, S., Peters, J., Hunter, A. & Martin, J. (1997) *Mamm. Genome* **8,** 711–713.
26. Lijam, N., Paylor, R., McDonald, M. P., Crawley, J. N., Deng, C. X., Herrup, K., Stevens, K. E., Maccaferri, G., McBain, C. J., Sussman, D. J., *et al.* (1997) *Cell* **90,** 895–905.
27. Crawley, J. N. (1999) *Brain Res.* **835,** 18–26.
28. Gao, J., Cheon, K., Nusinowitz, S., Liu, Q., Bei, D., Atkins, K., Azimi, A., Daiger, S. P., Farber, D. B., Heckenlively, J. R., *et al.* (2002) *Proc. Natl. Acad. Sci. USA* **99,** 5698–5703.
29. Cantiello, H. F. (2003) *Trends Mol. Med.* **9,** 234–236.
30. Kulaga, H. M., Leitch, C. C., Eichers, E. R., Badano, J. L., Lesemann, A., Hoskins, B. E., Lupski, J. R., Beales, P. L., Reed, R. R. & Katsanis, N. (2004) *Nat. Genet.* **36,** 994–998.